European Journal of Medicinal Chemistry 208 (2020) 112554

Contents lists available at ScienceDirect

European Journal of Medicinal Chemistry

journal homepage: http://www.elsevier.com/locate/ejmech

Research paper

Synthesis, bioevaluation and docking studies of some 2-phenyl-1*H*-benzimidazole derivatives as anthelminthic agents against the nematode *Teladorsagia circumcincta*

Nerea Escala [a, 1], Elora Valderas-García [b, c, 1], María Álvarez Bardón [b], Verónica Castilla Gómez de Agüero [c, d], Ricardo Escarcena [a], José Luis López-Pérez [a, e], Francisco A. Rojo-Vázquez [d], Arturo San Feliciano [a, f], Rafael Balaña-Fouce [b, **], María Martínez-Valladares [c, d, ***], Esther del Olmo [a, *]

[a] Departamento de Ciencias Farmacéuticas: Química Farmacéutica, Facultad de Farmacia, Universidad de Salamanca, CIETUS, IBSAL, 37007, Salamanca, Spain
[b] Departamento de Ciencias Biomédicas, Facultad de Veterinaria, Universidad de León, 24071, León, Spain
[c] Instituto de Ganadería de Montaña, CSIC-Universidad de León, 24346, Grulleros, León, Spain
[d] Departamento de Sanidad Animal, Facultad de Veterinaria, Universidad de León, 24071, León, Spain
[e] Facultad de Medicina, Universidad de Panamá, Panamá, R. de Panamá
[f] Programa de Pós-graduaçao em Ciências Farmacêuticas, Universidade do Vale do Itajaí, UNIVALI. Itajaí, SC, Brazil

ARTICLE INFO

Article history:
Received 10 April 2020
Received in revised form
3 June 2020
Accepted 7 June 2020
Available online 7 July 2020

Keywords:
2-Phenyl-1*H*-benzimidazoles
Teladorsagia circumcincta
in vitro assays
Cytotoxicity
Tubulin docking studies

ABSTRACT

Gastrointestinal nematode infections are the main diseases in herds of small ruminants. Resistance to the main established drugs has become a worldwide problem. The purpose of this study is to obtain and evaluate the *in vitro* ovicidal and larvicidal activity of some 2-phenylbenzimidazole derivatives on susceptible and resistant strains of *Teladorsagia circumcincta*. Compounds were prepared by known procedures from substituted *o*-phenylenediamines and arylaldehydes or intermediate sodium 1-hydroxyphenylmethanesulfonate derivatives. Egg Hatch Test (EHT), Larval Mortality Test (LMT) and Larval Migration Inhibition Test (LMIT) were used in the initial screening of compounds at 50 μM concentration, and EC_{50} values were determined for the most potent compounds. Cytotoxicity evaluation of compounds was conducted on human Caco-2 and HepG2 cell lines to calculate their Selectivity Indexes (SI). At 50 μM concentration, nine out of twenty-four compounds displayed more than 98% ovicidal activity on a susceptible strain, and four of them showed more than 86% on one resistant strain. The most potent ovicidal benzimidazole (BZ) **3** showed EC_{50} = 6.30 μM, for the susceptible strain, while BZ **2** showed the lowest EC_{50} value of 14.5 μM for the resistant strain. Docking studies of most potent compounds in a modelled *Teladorsagia* tubulin indicated an inverted orientation for BZ **1** in the colchicine binding site, probably due to its fair interaction with glutamic acid at codon 198, which could justify its inactivity against the resistant strain of *T. circumcincta*.

1. Introduction

Nematodes are roundworms belonging to the group of parasitic helminths that affect different host species, including humans and animals. Soil transmitted helminths (STH) infected more than one billion people around the world and contributed to 3.45 million disability adjusted life-years (DALYs) in 2016 [1]. Although these infections are more prevalent in low-income countries, they also occur in wealthy countries, such as the USA, Australia and some countries of the Mediterranean basin [2–4]. Moreover, infections produced by gastrointestinal nematodes (GIN)s are one of the most prevalent parasitic diseases affecting grazing ruminants worldwide. Their importance is due to the significant economic losses they produce as a result of decreased production and increased healthcare costs [5–7].

* Corresponding author.
** Corresponding author.
*** Corresponding author.
E-mail addresses: rbalf@unileon.es (R. Balaña-Fouce), mmarva@unileon.es (M. Martínez-Valladares), olmo@usal.es (E. Olmo).
[1] Both authors shared the first position.

https://doi.org/10.1016/j.ejmech.2020.112554
0223-5234/

The control of GIN infections is based on the strategic application of anthelmintic drugs, but their massive and incorrect administration have led to the development of anthelmintic resistance (AR), especially in ruminants. The emergence of AR has been described in the three classes of broad-spectrum anthelmintic drugs most commonly used in animals: benzimidazoles such as fenbendazole, mebendazole and albendazole, among others, macrocyclic lactones (MLs) such as ivermectin and moxidectin, and imidazothiazoles (IMs) such as levamisole [8–10]. Of these three classes of anthelmintic drugs, the BZ group that usually interferes tubulin polymerization and functions in parasites is the most popular and used in the control of GIN infections. Unfortunately, the current situation of resistance to this family of drugs in animals represents a serious problem for livestock production, mainly in sheep. This phenomenon is widely distributed, since resistant populations have been reported all over the world [11–14].

In humans, the World Health Organisation (WHO) recommends preventive chemotherapy, as a public health intervention to at-risk people living in endemic STH areas by mass administration of BZs, mainly albendazole or mebendazole. In consequence, there are already studies showing the decrease of BZ efficacy against some STH and the possible development of AR after years of mass drug administration campaigns [15].

It is well known that the mechanism of action of BZs is targeted to the selective binding of the high affinity colchicine site of parasite β-tubulin that prevents the formation of microtubules, which results in the destruction of cell structure and consequently in the death of the parasite [11]; in fact, competitive inhibition studies in mammalian isolated tubulins show that colchicine and BZ bind at the same site near the *N*-terminal domain [16]. Computational studies performed with BZs support this finding [17]. Three amino acid mutations (F167Y, E198A and F200Y) have been associated with major causes of anthelmintic drug resistance due to loss of drug affinity by β-tubulin [18], which seems to indicate that these amino acids would be located at or close to the colchicine binding site.

The problem of AR is seriously aggravated by the limited development of novel anthelmintic drugs during the last years. Classical BZ derivatives with nematocidal properties, such as albendazole, fenbendazole, mebendazole, oxibendazole, parbendazole or luxabendazole display a carbamate fragment at position C-2. Their activity is due to disruption of functions on the microtubule system [19]. The carbamate fragment can be substituted by an electron rich fragment such as a phenyl ring [20]. Here we report on the synthesis and bio-evaluation of some BZ derivatives containing a substituted phenyl group attached to the C-2 position of the benzimidazole system.

According to Zajíčková et al. [21] an effective approach to obtain new anthelmintics is to exploit the old ones, synthesizing derivatives and analogues of known drugs with an approved usage. Interestingly, although many 2-phenylbenzimidazole derivatives were synthesized and tested against viruses, fungi, and bacteria infecting humans or animals [22–24], and most rarely against helminths, no evaluation of BZs against *Teladorsagia circumcincta* could be found. In a previous study, the south Indian adult earth worm *Pheretima posthuma* was used as a model for testing the anthelmintic activity of 2-phenylbenzimidazole derivatives [25]. However, it is important to note that *P. posthuma* is not a parasitic worm, does not belong to phylum Nematoda, and therefore it is not the most suitable model for parasitic infections.

In this context, the goal of the present study is to synthesize several series of BZ derivatives, aiming to obtain new drugs with improved therapeutic profiles compared to those already marketed, as well as to evaluate *in vitro* their anthelmintic activity against *Teladorsagia circumcincta*, which is a good experimental model for sheep parasitic nematode infections, as well as one of the most prevalent GIN species in small ruminants worldwide, specifically in template areas [26]. Our research includes *in vitro* cytotoxicity tests in order to define candidate molecules for *in vivo* efficacy and toxicity assays. With these aims, the anthelmintic activity has been assessed in three life-cycle stages (eggs and larvae at two levels of growth) of *Teladorsagia circumcincta*, by means of assaying the BZs on two isolates, one susceptible and the other resistant to marketed drugs as albendazole, levamisole and ivermectin. The cytotoxicity evaluation has been carried out on Caco-2 (human colorectal adenocarcinoma) and the HepG2 (hepatocarcinoma) cells.

2. Results and discussion

2.1. Chemistry

Ten BZ derivatives were obtained by a reported two steps procedure. First, the sodium 1-hydroxyphenylmethanesulfonate derivatives were prepared from the corresponding aldehydes, and then coupled with substituted *o*-phenylenediamines in *N*,*N*-dimethylformamide (DMF) at 110–120 °C, to provide the desired BZs in 43–87% yield [27]. Eleven BZs were obtained in a single step by direct condensation of 1,2-phenylenediamines with the corresponding benzaldehyde derivative in DMF and in the presence of sodium metabisulfite ($Na_2S_2O_5$) under reflux for 16–20 h [28], (Scheme 1). The wide range of yields observed in these syntheses is similar or even lower than those reported by other authors. It can be mainly justified by the diverse electronic nature of the substituents and the influence of their inductive and mesomeric effects on the electrophilia of the aldehyde carbonyl or on the sulfonate α-carbon, and at a lesser level by the nucleophilia of the amino groups. Actually, when the substituents involved are *p*-Cl and the *m*-NO_2 groups at ring B, the yields are the highest.

The original articles referenced above comprise proposals for the reaction mechanisms involved in these BZ syntheses. More recently, Penieres-Castillo et al. [29] have published a more complete study on the subject in which they described different reaction conditions.

BZs **13** and **18** were obtained by reduction of the corresponding nitrobenzimidazoles with H_2 under Pd–C catalysis, while BZ **19** was obtained in 70% yield from the amine **18** by reaction with picolinic acid in the presence of 1,1-carbonyldiimidazole (CDI) as coupling agent. Scheme 2.

Physicochemical, MS and NMR spectral data for all the BZs are reported in the experimental section. IR spectra of BZs showed strong or very strong stretching (*str*) absorption bands of the benzimidazole moiety near 3315 (N–H), 1613 and 1535 (Ar C–C), 1460 and 1384 (C=N) cm^{-1}; along with those associated to the substituents on rings A and B, near 1521 and 1349 cm^{-1} (NO_2 *asym* and *sym str* bands, respectively), 1255 cm^{-1} (C–O), 731 cm^{-1} (C–Cl), 679 cm^{-1} (C–Br) or 1663 cm^{-1} (HN–C=O amide I *str* band). NMR spectra were run either in methanol-d_4 or DMSO-d_6. ^1H NMR and ^{13}C NMR spectra of BZs **1**, **2**, **3**, **23** and **24** resulted simplified due to the symmetry of their structures. As an example, in the ^1H NMR spectrum of BZ **1,** five signals were appreciated; one singlet at 3.84 ppm, corresponding to the methoxy group; two doublets ($J = 8.6$ Hz) at 7.06 and 7.99 ppm, that correspond to H-3′+5′and H-2′+6′, respectively, and two multiplets at 7.23 and 7.56 ppm corresponding to H-5+6 and H-4+7, respectively. With respect to the ^{13}C NMR spectrum eight signals were observed, one of a $O\underline{C}H_3$ at 54.5 ppm, three of aromatic methines at 114.1 (~double intensity),

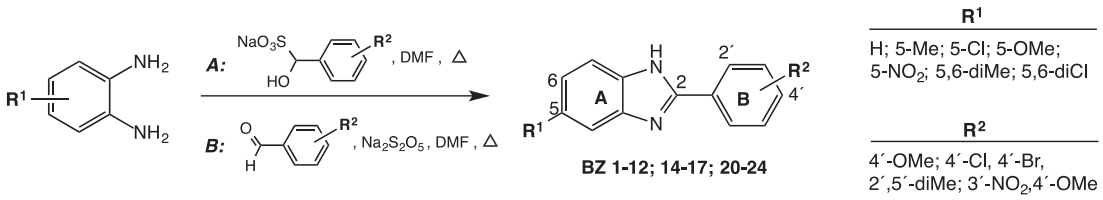

Scheme 1. Two procedures for the synthesis of 2-phenylbenzimidazole derivatives.

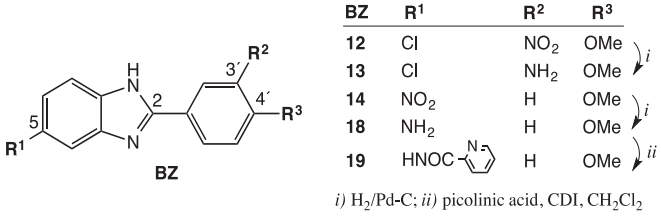

Scheme 2. The preparation of BZs 13, 18 and 19.

122.4 and 128.0 ppm assigned to C-3′+5′and C-4+7, C-5+6 and C-2′+6′, respectively, and four of non-protonated carbons at 121.7, 138.5, 152.0 and 161.7 ppm, corresponding to C-1′, C-3a+7a, C-2 and C-4′, respectively. Regarding ^{1}H NMR spectra of 5-substituted BZs, the signals corresponding to different protons were assigned taking into account their splitting patterns and chemical shifts. Related to the benzimidazole fragment, the signal corresponding to proton H-4 resonates in the 7.1–7.6 ppm range. The chemical shift corresponding to H-6 appears at 7.1–7.4 ppm, except in the presence of nitrogen substituents, such as NO_2 (fairly downfield, ~8.2 ppm), NH_2 (fairly upfield, 6.7 ppm) or NHCO (slightly downfield, 7.5 ppm). The signal for H-7 resonates in the 7.4–7.6 ppm interval, though with changes similar to those just above indicated in presence of nitrogen substituents. ^{13}C NMR spectra of 5-substituted BZs, related to the benzimidazole fragment, showed signals of four non protonated carbons, C-2 (150–157 ppm), C-5 (127–158 ppm), C-3a (131–141 ppm) and C-7a (132–147 ppm). Related the last two carbons, low and broad signals were observed in some spectra due to poor relaxation caused by their proximity to nitrogen atoms. Additionally, the signals of three methines C-4 (96–116 ppm), C-6 (113–124 ppm) and C-7 (112–116 ppm) were appreciated. Chemical shifts of the signals corresponding to ring B were also appropriately assigned considering the substitution pattern of that ring.

2D-NMR experiments on BZ **19** allowed the assignment of the additional signals corresponding to the pyridine portion. In the ^{1}H NMR spectrum, those multiplets at 7.62, 8.23, 8.29 and 8.73 ppm, corresponding to H-5, H-4, H-3 and H-6, respectively, are correlated with signals at 127.9, 139.1, 123.3 and 149.7 ppm, respectively in the ^{13}C NMR spectrum.

2.2. Biological assays

2.2.1. Anthelmintic activity and toxicity

All the compounds synthesized according to Schemes 1 and 2 were tested against a susceptible strain of *T. circumcinta* and their ovicidal (egg hatching inhibition) effects were determined (see Table 1). Those compounds showing ovicidal activity >98% were also tested against one resistant strain. Cytotoxicity was assessed on human Caco-2 and HepG2 cells cultures. Compounds listed in Table 1 are organized in first place by the number and type of substituents at position C-5 (C-6) of the benzimidazole system, and second, by the substituents on the 2-phenyl ring. From the results included in Table 1, it can be observed that several compounds displaying R^1 = H, Me, OMe or Cl, in combination with R^2 = 4-OMe, 4-Cl or 4-Br showed both inhibitory effects, on egg hatching (EHT) and on larvae motility (LMT) at 50 μM final concentration. Notably, nine BZs displayed their anti-hatching effect between 98.2 and 100% on the susceptible strain, and five of them showed this effect between 81.1 and 98.9% on the resistant strain. Additionally, two BZs caused the death of first stage larvae (L1) at 50 μM. On the other hand, compounds with polar groups such as NO_2, NH_2 or picolinamido in R^1, did not show a measurable effect on the nematodes, nor on the susceptible or the resistant strain. Similarly, double substitutions on ring A, as those 5,6-dimethyl (BZ **23**) or 5,6-dichloro (BZ **24**), also led to inactivity.

It is also interesting to verify that the type of substituent on C-4′ of the B-phenyl ring conditioned the anthelmintic potency of active compounds. Curiously, some substituents as $-OCH_3$ and -Cl displayed higher effects at such 4′-position than if they are attached to the BZ moiety. Thus, with respect to ring A, the unsubstituted BZs **1**, **2** and **3**, the 5-CH_3 (BZs **4** and **5**), the 5-Cl (BZs **8** and **9**) and the 5-OCH_3 (BZs **21** and **22**) were able to arrest the hatching of wild-type *T. circumcinta* eggs in more than 98% at the pre-established 50 μM concentration. Among them, the BZs **2**, **4**, **8**, **9** and **22** were also able to produce a significant hatching inhibition on eggs, between 81.1 and 98,9%, of the resistant strain of *T. circumcincta* used in this study. Surprisingly, despite its structural similarity with the most potent substances in the series, BZ **1** is the only one that loses much of its inhibitory capacity against the resistant strain.

Egg-hatching dose/response curves of the compounds of interest were performed in at least 6 final concentrations in order to determine an EC_{50} value that could be comparable with mammalian cytotoxicity (in the Supporting Information). Eight out of the nine hits mentioned above showed similar EC_{50} values within the 6.30–15.78 μM range. The most effective ovicidal BZs were **3** and **9**, which displayed significantly low EC_{50} values of 6.30 and 6.54 μM, respectively, that is, around 14 times less active than thiabendazole. The EC_{50} values of the most potent compounds on the resistant strain ranged between 14.47 and 25.76 μM, which are 9 and 17 times less active than the reference drug, respectively.

When analysing the effect of this series of 2-phenyl benzimidazole compounds on mammalian cells, all the compounds were significantly cytotoxic within a range of 9.07–83.17 μM. Considering only those compounds that have a significant effect against *T. circumcincta*, namely BZs **1**–**5**, **8**, **9**, **21** and **22**, their CC_{50} values were very homogeneous between Caco-2 and HepG2. This determined the SI values calculated for these compounds in the susceptible strain of the parasite to be comprised between 6.22 (BZ **3**) and 0.95 (BZ **4**) for Caco-2 cells and 6.22 (BZ **3**) and 0.87 (BZ **22**) for HepG2 cells. In the case of the resistant strain, the SI values were slightly lower and are comprised between 2.94 (BZ **2**) and 0.47 (BZ **4**) for the Caco-2 cells and between 3.56 and 0.76 for the same compounds and HepG2 cells.

In order to study the killing effect of the twenty-four compounds

Table 1
Inhibitory effects of BZs on hatching of wild type and resistant eggs of *Teladorsagia circumcinta*. Cytotoxicity and selectivity indexes.

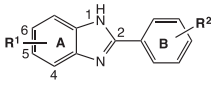

Compound			*T. circumcincta* susceptible strain		*T. circumcincta* resistant strain		Cytotoxicity [a] CC_{50}, μM		Selectivity Indexes[b]			
BZ	R^1	R^2	Hatch inhib. % at 50 uM	Ovicidal EC_{50}, μM	Hatch inhib. % at 50 μM	Ovicidal EC_{50}, μM	Caco-2	HepG2	SIs Caco-2	SIr Caco-2	SIs HepG2	SIr HepG2
1	H	4-OMe	**100**	**15.78 ± 0.12**	18.2	> 50	56.80 ± 8.12	43.08 ± 3.42	3.60	< 1	2.73	< 1
2	H	4-Cl	**99.5**	**9.04 ± 0.23**	**86.4**	**14.47 ± 1.05**	42.63 ± 6.50	51.46 ± 6.27	**4.72**	2.94	**5.69**	3.56
3	H	4-Br	**99.8**	**6.30 ± 0.23**	65.8	< 50	39.17 ± 2.46	38.36 ± 2.36	**6.22**	nc	**6.09**	nc
4	5-Me	4-OMe	**100**	**12.21 ± 0.29**	**81.1**	24.80 ± 0.99	11.60 ± 3.42	18.75 ± 1.92	0.95	0.47	1.53	0.76
5	5-Me	4-Cl	**99.5**	**15.23 ± 0.78**	71.8	< 50	28.06 ± 1.35	27.11 ± 1.69	1.84	< 1	1.78	< 1
6	5-Me	2,5-diMe	0,80	> 50	na	nc	9.14 ± 2.32	> 25	nc	nc	nc	nc
7	5-Me	3-NO_2,4-OMe	1.11	> 50	na	nc	9.07 ± 2.35	> 25	nc	nc	nc	nc
8	5-Cl	4-OMe	**100**	**13.74 ± 0.46**	**89.6**	25.76 ± 3.48	37.38 ± 3.38	36.03 ± 3.02	2.72	1.45	2.62	1.39
9	5-Cl	4-Cl	**99.6**	**6.54 ± 0.40**	**94.0**	20.90 ± 0.50	22.58 ± 1.69	17.54 ± 0.91	3.45	1.08	2.68	0.84
10	5-Cl	4- NO_2	1.25	> 50	na	nc	19.14 ± 2.05	21.73 ± 1.65	nc	nc	nc	nc
11	5-Cl	2,5-diMe	4.00	> 50	na	nc	23.28 ± 2.47	30.22 ± 3.35	nc	nc	nc	nc
12	5-Cl	3-NO_2,4-OMe	0.97	> 50	na	nc	67.31 ± 15.31	53.43 ± 16.61	nc	nc	nc	nc
13	5-Cl	3-NH_2,4-OMe	1.00	> 50	na	nc	34.70 ± 4.32	44.91 ± 5.94	nc	nc	nc	nc
14	5-NO_2	4-OMe	3.16	> 50	na	nc	14.37 ± 3.69	22.98 ± 19.57	nc	nc	nc	nc
15	5-NO_2	4-Cl	1.61	> 50	na	nc	12.29 ± 1.09	14.64 ± 0.83	nc	nc	nc	nc
16	5-NO_2	2,5-diMe	4.02	> 50	na	nc	16.78 ± 9.16	> 12.5	nc	nc	nc	nc
17	5-NO_2	3-NO_2,4-OMe	0.88	> 50	na	nc	13.38 ± 3.02	13.64 ± 4.85	nc	nc	nc	nc
18	5-NH_2	4-OMe	0.50	> 50	na	nc	> 25	> 50	nc	nc	nc	nc
19	5-NHpic [c]	4-OMe	17.1	> 50	na	nc	83.17 ± 45.84	22.76 ± 2.08	nc	nc	nc	nc
20	5-OMe	4-OMe	44.1	> 50	na	nc	21.80 ± 1.47	19.11 ± 3.68	nc	nc	nc	nc
21	5-OMe	4-Cl	**98.2**	25.60 ± 1.25	70.6	< 50	28.94 ± 1.47	21.33 ± 1.20	1.13	nc	0.83	nc
22	5-OMe	4-Br	**99.9**	**15.34 ± 0.55**	**98.9**	**15.99 ± 0.42**	21.69 ± 1.61	13.48 ± 0.64	1.41	1.36	0.87	0.84
23	5,6-diMe	4-OMe	17.4	> 50	na	nc	13.01 ± 1.23	31.66 ± 4.09	nc	nc	nc	nc
24	5,6-diCl	4-OMe	0.44	> 50	na	nc	16.68 ± 1.46	26.37 ± 2.29	nc	nc	nc	nc
Thiabendazole (TBZ)			100	0.43 ± 0.02	100	1.53 ± 0.06	> 300	>300	>697	>196	>697	>196

[c] picolinamide; *na*: not appreciable; *nc*: not calculated. Hatching inhibition values > **80%** and > **90%**, the EC_{50} values < **10** and < **20** μM, and the SI values > **4** have been bolded to facilitate comparisons.
[a] Determined by the Alamar Blue method.
[b] Selectivity index: SI = CC_{50}(Caco-2 or HepG2)/EC_{50}(*T.c.*), relative to susceptible (SIs) and resistant (SI*r*) strains.

on both susceptible and resistant *T. circumcincta* L1, we used the LMT assay with levamisol (LEV) as reference drug for comparison. Interestingly, three compounds of this series showed activity at this stage of the parasite: BZ **4** with a larvicidal activity higher than 40%, and BZ **9** and **22**, with lesser cytotoxicity which produced 100% death of susceptible L1 larvae of *T. circumcincta*. Table 2 includes the larvicidal results showing that these compounds proved much more potent than LEV, and in the case of BZ **9** also fairly more selective. Nevertheless, it must be taken into account that SI*s,r* values in Table 2 are just indicative, because they were calculated using the cytotoxicity CC_{50} values on human cells, whereas the EC_{50} values were determined on a complete and living organism, the nematode larvae. Independently, the SI is a useful parameter to compare the relative toxicities and selectivities of BZs with those of the currently used anthelmintic drug LEV. The EC_{50} values for susceptible L1 were 5.01 and 28.06 μM for BZs **9** and **22**, respectively (see also Supporting Information). The activity of BZ **9** on larvae was much potent than on *Teladorsagia* eggs, while the activity of BZ **22** was more potent on *Teladorsagia* eggs.

Very interestingly, as it can be seen in Table 2, BZs **9** and **22** killed practically all L1 larvae of both susceptible and resistant strains at 50 μM, with EC_{50} values in de low-medium μM range. Furthermore, both BZs were fairly more potent than the reference drug LEV, and BZ **9**, the most active compound, also showed higher SI values than LEV.

The effect of the compounds against the infective form of the parasite, third stage larvae (L3), was assessed using the LMIT assay. The results showed that they did not produce a significant inhibition of motility, since the highest percentage of inhibition of L3 migration was barely 30% in the case of BZ **23**.

In order to analyze the drugability of the active BZs, a preliminary prediction study was performed online through the Osiris Data Warrior and preADMET free web services (see Experimental section *4.2.6* for details. Detailed results are shown in Table S1 of Supporting Information). To sum up, all the active BZs fulfil Lipinski's Rule of Five with MW values in the range of 224.3–303.2 amu, clogP values between 2.8 and 4.1, and the H-bond acceptors and donors (2–3 and 1, respectively) under the established limits. Other properties as their solubility (>1–100 μM), total and polar surfaces (171–196 and 28–38 $Å^2$, respectively), very good intestinal absorption (>92%) and plasma protein binding (<90%) ensuring their distribution, as well as their qualification within the 90% cut-off in the World Drug Index, contributed to configure their Drug Score values in the range 0.40–0.69 of the Osiris algorithm. Most significantly, none of the active BZs was predicted to show any of those toxicity risks, mutagenic, tumorigenic, reproductive effective or irritant effects, considered in the Osiris panel.

2.3. Molecular docking studies

In order to justify the differential activity of these compounds against susceptible and resistant strains of *T. circumcincta* and further understand the molecular basis of its inhibitory properties, all compounds described in this study were subjected to molecular docking with the *T. circumcincta* tubulin, previously obtained by homology modelling as described in the experimental section *4.2.7*.

Table 2
Larvicidal effects of active BZs on susceptible and resistant larvae of *Teladorsagia circumcincta*.

	T. circumcincta L1 susceptible strain		*T. circumcincta* L1 resistant strain		Cytotoxicity [a]	Selectivity Indexes [b]
BZ	Mortality % at 50 μM	Larvicidal EC_{50} μM	Mortality % at 50 μM	Larvicidal EC_{50} μM	SIs Caco-2	SIr Caco-2
4	40.9	> 50	*nt*	*nd*	0.95	0.47
9	100	**5.01 ± 0.04**	100	**11.66 ± 0.21**	**4.51**	1.94
22	100	**28.06 ± 2.95**	99.3	**28.99 ± 3.32**	0.77	0.75
LEV	0	1782 ± 26	0	2410 ± 23	1.63	1.20

[a,b] reproduced from Table 1 for comparison with the reference drug levamisol (LEV). SI = CC_{50}(Caco-2) / EC_{50}(L1). *s,r*: related to L1 of susceptible and resistant strains, respectively. *nd:* not determined. *nt*: not tested. EC_{50} values <**10** and <**30** μM and SI values >**4** have been bolded to facilitate comparisons.

Taking into account the possibility of tautomerism of the benzimidazole system, which may lead to mixtures in dynamic equilibrium of asymmetrically substituted compounds, computational calculations at the DFT level, MN15/6-31+G(d,p), as described in the experimental section *4.2.8* were conducted with the most potent BZs of this study. The results obtained indicate that the tautomer with the substituent at C-6 (**B**) is about 0.5–1 kcal/mol more stable than the substituent at C-5 (**A**) (Scheme 3).

The activity ranking of the docked compounds of Table 1 in the mentioned *T. circumcincta* tubulin homology model is in agreement with the ovicidal EC_{50} results. In fact, all BZs that show a value of EC_{50} in the μM range (Table 1) appear positioned in the first places of the energetic ranking according the GlideScore function implemented in GLIDE (*see* section 4.2.8). Interestingly, the active conformation of the most efficient compounds corresponds to that of the lowest energy tautomer. The docking poses of some significant ligands can be visualized in Fig. 1 and 2 D maps of interactions in Fig. 2 and Supporting Information p. S41.

Looking at the docked molecules of Fig. 1 and the 2D-maps of tubulin-BZs interactions of Fig. 2, it can be seen that with the exception of BZ **1,** the active compounds are arranged with the same orientation in the site, while other aspects can be deduced from deeper examinations. Experimentally active ligands have none or only one substituent in the benzene ring of the benzimidazole system, whereas the presence of two substituents results in a loss of activity. Those with only one substituent bind tubulin through the lowest energy tautomer; that is, with the substituent located at C-6 according to the systematic IUPAC numbering. The possibility of interaction of the ligands in the tautomer substituted at C-5 results unfavourable due to the steric effect exerted by the methyl group of Ala314. This effect is clearly evident in 5,6-disubstituted BZs, as for example, in the cases of the BZ pairs **4**/**23** or **8**/**24**. A decrease in potency is also observed in those BZs with the potent electron attracting substituent $-NO_2$ located on any benzene ring. This group is placed in an unfavourable hydrophobic environment and provokes bad contacts with several amino acids of the binding site (Fig. 3).

In the colchicine binding site, the active compounds commonly establish a hydrogen bond with the peptide carbonyl of Val236 through their BZN-H acting as a donor. Additionally, some of the most potent compounds present π-stacking interactions between the BZ moiety and the tubulin Phe200 (Fig. 4).

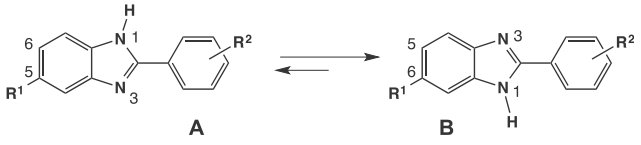

Scheme 3. Tautomeric equilibrium shift and systematic numbering for non-symmetrically 5(6)-monosubstituted BZs.

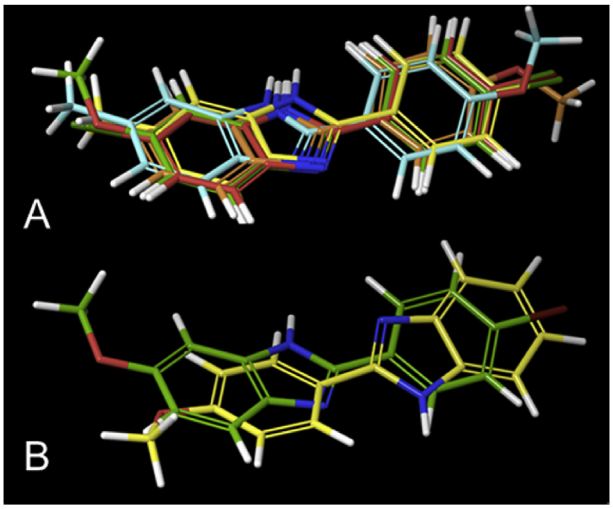

Fig. 1. A: Superimposition of the most potent BZs (**4**: cyan, **5**: yellow, **8**: brown **9**: red, and **22**: green) **as docked in the colchicine site of the *T. circumcincta* tubulin model. B: Superimposition of docked BZs 1** (yellow) **and 22** (green). (For interpretation of the references to color in this figure legend, the reader is referred to the Web version of this article.)

Interestingly, as shown in Figs. 1, 2 and 4, BZ **1** without any substituent on ring A interacts with tubulin in an inverse arrangement with respect to most compounds of the series, (also BZ **8** in Supporting Information, p. S41). As a consequence, it establishes its own BZN-H bond with the γ-carboxyl group of Glu198 instead of the amide carbonyl of Val236. Most of BZs establish a common H-bond acceptor with Val236 and also display π-stacking interactions with the phenyl group of Phe200 through its imidazole nucleus (Fig. 4). This different model of interaction could account for the loss of activity of this compound against resistant strains. Indeed, as described in the literature [18], the mutations associated with BZ-resistant strains for *T. circumcincta* and *Haemonchus contortus* are actually Phe167Tyr, Glu198Ala and Phe200Tyr, and as shown graphically and stated above, Glu198 and Phe200 are directly involved in tubulin - BZs interactions, which should result perturbed in some extension by such mutations.

3. Conclusions

In summary, we have identified some 2-phenylbenzimidazoles that exhibit promising nematocidal activity. Nine compounds displayed more than 98% ovicidal activity on *T. circumcincta* susceptible strain at 50 μM, and five of them showed more than 80% ovicidal activity on a resistant strain of *T. circumcincta* at the same concentration. BZ **3** was the most potent ovicidal on the susceptible strain, with an EC_{50} value of 6.30 μM and SI of 6.22 in relation to Caco-2 cells. BZ **2**, showed the lowest EC_{50} value of 14.47 μM on the

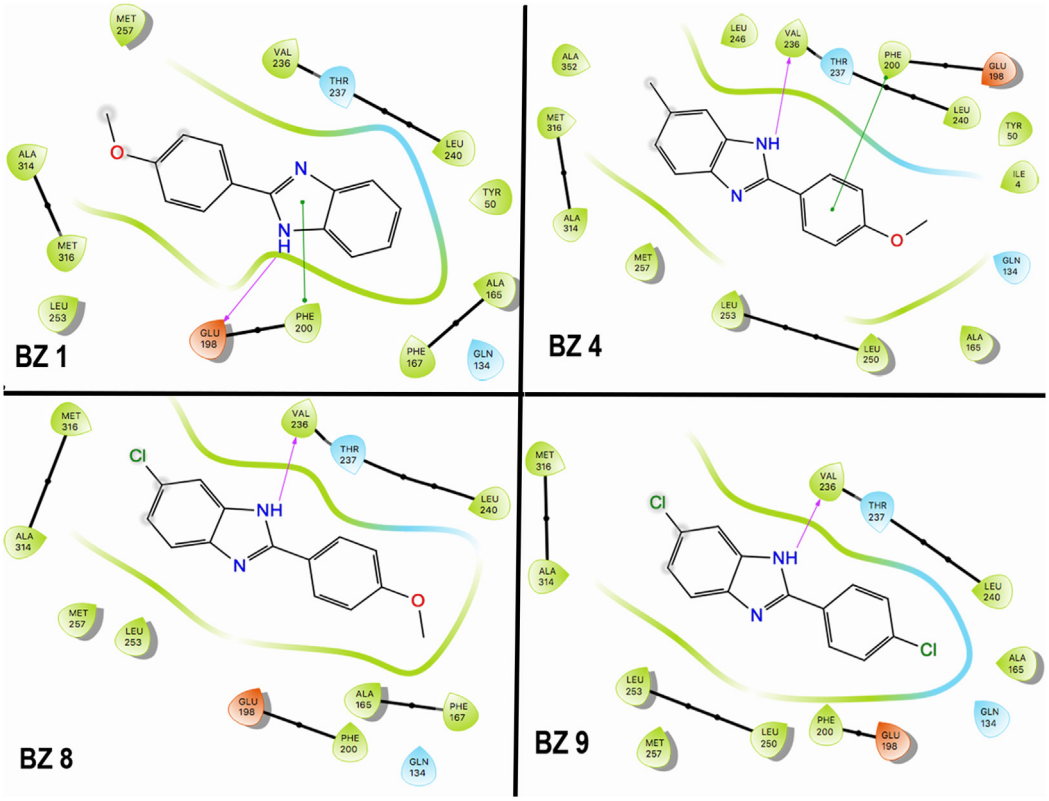

Fig. 2. 2D interaction maps resulting from the docking studies of several selected compounds at the colchicine site of *T. circumcincta* tubulin model. (For other 2D maps, see suppl. info).

resistant strain and SI of 2.94 on Caco-2 cells. Two BZs produced the motility inhibition and death of *T. circumcincta* L1, though none of them showed significant motility inhibition on the L3 stage. Docking studies of most active BZs on a modelled tubulin of *T. circumcincta* indicated a steric orientation of BZs **1** and **8** in their interaction with tubulin, that fairly differ from the other BZs of this study, and that could justify the lack of effect of BZ **1** against the resistant strain of *T. circumcincta.* Globally, these results do not seem very good, mainly because the infective L3 larvae were resistant to the 24 BZs assayed, however, they constitute a promising starting point to design and synthesize other compounds with improved tubulin affinity and higher antiparasitic efficacy.

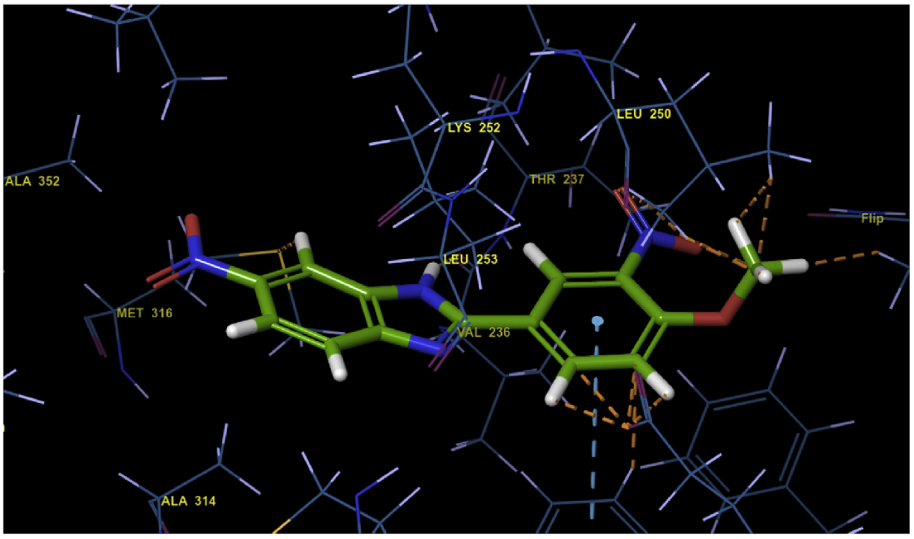

Fig. 3. Bad contacts (pink broken lines) **of nitro and methoxy groups of BZ 17.** (For interpretation of the references to color in this figure legend, the reader is referred to the Web version of this article.)

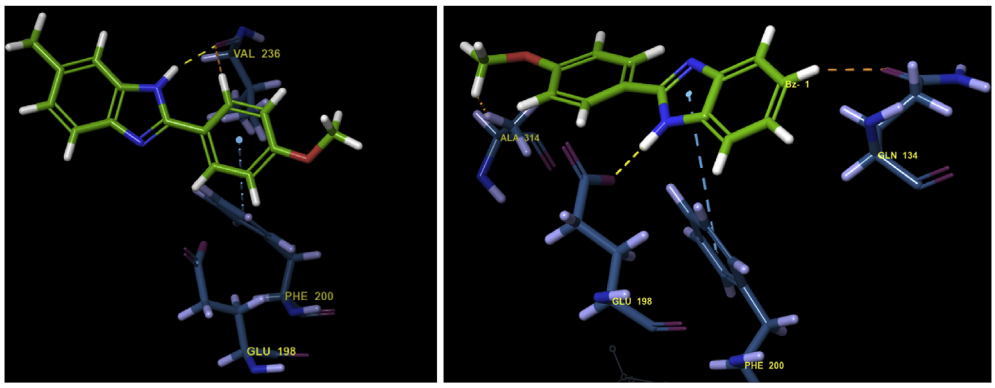

Fig. 4. BZ 4 establishes a hydrogen bond (yellowish broken line) **between its 1-BZN-H and the amide carbonyl of Val236** (*left*)**, while BZ 1 establishes the hydrogen bond with Glu198** (*right*).

Preliminarily, supported by its activity/selectivity profile and acceptable ADME/toxicity-risks predictions, BZ **9** could be selected for *in vivo* efficacy and acute toxicity evaluation on infected laboratory animals. The combined use of BZ **9** and other approved anthelminthic agent acting through a different mechanism against the parasite, also looking for additive or synergic effects could also be considered. However, further and more complete research will be first carried out to obtain better candidates with effects on L3 larvae, with a greater nematocidal potency and a higher selectivity index.

4. Experimental

4.1. Chemistry

4.1.1. Chemistry general

All commercial chemicals (Aldrich, Alpha, Fischer, SDS) were used as purchased and solvents (Fischer, SDS, Scharlau) purified by the standard procedures prior to use [30]. Reactions were monitored by Thin Layer Chromatography (TLC) (Kieselgel 60 F254 precoated plates, E. Merck, Germany), the spots were detected by exposure to UV light at λ 254 nm, and colorization with 10% ninhydrin spray, and further heating of the plate. Melting points (Mp) were determined with a Büchi apparatus in open capillaries and were uncorrected. Separations by flash column chromatography were performed on Merck 60 silica gel (0.063–0.2 mesh). Infrared spectra were recorded on a FT-IR spectrometer PerkinElmer, System BX using solid samples in KBr disks. NMR spectra were recorded on a Bruker Avance 400 MHz (400 MHz for ^{1}H, 100 MHz for ^{13}C) and Varian Mercury 200 MHz ((200 MHz for ^{1}H, 50 MHz for ^{13}C). The spectra were measured either in methanol-d_6 or DMSO-d_6, using tetramethylsilane (TMS) as internal standard, chemical shifts (δ) are given in ppm and coupling constants (J) in Hertz. High resolution mass spectra (HRMS) were obtained by electron spray ionisation-mass spectrometry (ESI-MS) technique (5 kV) on a QSTAR XL mass spectrometer.

4.1.2. Synthesis

4.1.2.1. Method A. General procedure for the synthesis of intermediate sodium hydroxy-(4-methoxyphenyl)methanesulfonate, ***SMS-1***. 4-methoxybenzaldehyde (7.34 mmol) and ethanol (22 mL) were added to a round-bottom flask equipped with a magnetic stir bar under argon atmosphere; then a 16% solution of $Na_2S_2O_5$ (5 mL) was added. The reaction mixture was vigorously stirred for 1 h at room temperature, and kept overnight a 4 °C in a refrigerator. The resulting precipitate was filtered off under vacuum to obtain a white solid in quantitative yield.

4.1.2.1.1. Sodium hydroxy-(4-methoxyphenyl)methanesulfonate, ***SMS-1***. White crystalline solid (100% yield); thermal decomposition of the compound prohibits melting point measurement. IR (KBr), ν_{max}: 3435, 3200, 2980, 1610, 1517, 1250, 1114, 839 cm^{-1}. ^{1}H NMR (C_2D_6SO): δ 3.70 (s, 3H), 4.85 (d, J = 5.0 Hz, D_2O, 1H), 5.65 (d, J = 5.0 Hz, 1H), 6.77 (d, J = 8.6 Hz, 2H), 7.31 (d, J = 8.6 Hz, 2H). ^{13}C NMR (C_2D_6SO): δ55.8, 83.7, 114.5 (2C), 128.1 (2C), 133.2, 159.2. HRMS (ESI$^+$) calcd. for $C_8H_9Na_2O_5S$[M+Na]$^+$: 262.9961; found: 262.9959.

4.1.2.1.2. Sodium hydroxy-(4-chlorophenyl)methanesulfonate, ***SMS-2***. White crystalline solid (100% yield); thermal decomposition of the compound prohibits melting point measurement. IR (KBr): ν_{max} 3440, 2930, 1660, 1595, 1244, 1136, 832, 621 cm^{-1}. ^{1}H NMR (C_2D_6SO): δ 4.91 (d, J = 5.4 Hz, D_2O, 1H), 5.94 (d, J = 5.4 Hz, 1H), 7.26 (d, J = 8.4 Hz, 2H), 7.41 (d, J = 8.4 Hz, 2H). ^{13}C NMR (C_2D_6SO): δ 84.2, 126.8 (2C), 129.5 (2C), 131.2, 138.8. HRMS (ESI$^+$) calcd. for $C_7H_7ClNaO_4S$ [M+Na]$^+$: 266.9465, found: 266.9462.

4.1.2.2. General procedure for the preparation of 2-phenylbenzimidazole derivatives from intermediates ***SMS-1*** *and* ***SMS-2*** *(compounds* ***1***, ***2***, ***4***, ***5***, ***8***, ***9***, ***14***, ***15***, ***23*** *and* ***24****).* 0.82 mmol of the corresponding intermediate was dissolved in *N*,*N*-dimethylformamide (2 mL) and 0.58 mmol of the substituted 1,2-phenylenediamine was added. The mixture was heated at 110–120 °C for 20–24 h with magnetic stirring. After cooling, the reaction crude was poured on a mixture of ice/water (150 mL) to give a solid that was filtered off in a Büchner funnel. The resulted solid was purified by column chromatography on silica gel with solvent gradient (hexane/ethyl acetate from 9:1 to 8:2), and recrystallized from the adequate solvent. Reaction yields ranged within 43–87%.

*4.1.2.2.1. 2-(4-Methoxyphenyl)-1*H*-benzimidazole,* **1**. Yield: 43%. Compound crystallized from EtOH to give a yellow solid, Mp: 229–230 °C. IR (KBr): ν_{max} 3460, 2836, 1611, 1436, 1254, 1179, 1035, 836, 803, 744 cm^{-1}. ^{1}H NMR (400 MHz, CD_3OD): δ 3.84 (s, 3H), 7.06 (d, J = 8.6 Hz, 2H), 7.23 (m, 2H), 7.56 (m, 2H), 7.99 (d, J = 8.6 Hz, 1H). ^{13}C NMR (100 MHz, CD_3OD): δ 54.5 ($O\underline{C}H_3$), 114.1 (C-4 + C-7 + C3' + C-5′), 121.7 (C-1′), 122.4 (C-5 + C-6), 128.0 (C-2′ + C-6′), 138.5 (C3a + C-7a), 152.0 (C-2), 161.7 (C-4′). HRMS (ESI$^+$) calcd. for $C_{14}H_{13}N_2O$ [M+H]$^+$: 225.1028, found: 225.1027.

4.1.2.2.2. 2-(4-Chlorophenyl)-1H-benzimidazole, **2**. Yield: 65%. Compound crystallized from EtOH to give a white solid, Mp: 300–301 °C. IR (KBr): ν_{max} 3459, 2920, 1611, 1429, 1272, 1176, 1089, 831, 803, 745 cm^{-1}. ^{1}H NMR (400 MHz, CD_3OD): δ 7.27 (m, 2H), 7.57 (d, J = 8.0 Hz, 2H), 7.61 (m, 2H), 8.06 (d, J = 8.0 Hz, 2H). ^{13}C NMR (100 MHz, CD_3OD): δ 124.2 (2C), 129.3 (4C), 129.6, 130.4 (2C), 137.4 (3C), 152.2. HRMS (ESI$^+$) calcd. for $C_{13}H_{10}ClN_2$ [M+H]$^+$: 229.0533, found: 229.0536.

4.1.2.2.3. 2-(4-Methoxyphenyl)-5-methyl-1H-benzimidazole, **4**. Yield: 59%. Compound crystallized from EtOH to give a light yellow solid, Mp: 163–164 °C. IR (KBr): ν_{max} 3460, 2921, 1611, 1438, 1255, 1176, 1030, 836, 803, 738 cm^{-1}. ^1H NMR (200 MHz, CD_3OD): δ 2.46 (s, 3H), 3.87 (s, 3H), 7.07 (d, J = 8.6 Hz, 2H), 7.08 (d, J = 8.2 Hz, 1H), 7.36 (bs, 1H), 7.44 (d, J = 8.2 Hz, 1H), 7.99 (d, J = 8.6 Hz, 2H). ^{13}C NMR (50 MHz, CD_3OD): δ 20.3 ($\underline{C}H_3$), 54.4 (O$\underline{C}H_3$), 113.6 (C-7), 114.0 (C-4 + C-3′ + C-5′), 122.0 (C-1′), 123.7 (C-6), 127.8 (C-2′ + C-6′), 132.1 (C-5), 137.2 (C-7a), 138.6 (C-3a), 151.8 (C-2), 161.4 (C-4′). HRMS (ESI^+) calcd. for $C_{15}H_{15}N_2O$ $[M+H]^+$: 239.1184, found: 239.1180.

4.1.2.2.4. 2-(4-Chlorophenyl)-5-methyl-1H-benzimidazole, **5**. Yield: 87%. Compound crystallized from EtOH to give a white solid, Mp: 189–190 °C. IR (KBr): ν_{max} 3580, 2921, 1630, 1520, 1418, 1090, 965, 834, 801, 731, 676 cm^{-1}. ^1H NMR (200 MHz, CD_3OD): δ 2.46 (s, 3H), 7.10 (dd, J_1 = 7.8; J_2 = 1.0 Hz, 1H), 7.38 (d, J = 1.0 Hz, 1H), 7.47 (d, J = 7.8 Hz, 1H), 7.52 (d, J = 9.0 Hz, 2H), 8.02 (d, J = 9.0 Hz, 2H). ^{13}C NMR (50 MHz, CD_3OD): δ 20.3, 113.8, 114.4, 124.4, 127.7 (2C), 128.2, 128.9 (2C), 133.0, 135.8, 137.0, 138.4, 150.3. HRMS (ESI^+) calcd. for $C_{14}H_{12}ClN_2$ $[M+H]^+$: 243.0689, found: 243.0687.

4.1.2.2.5. 5-Chloro-2-(4-methoxyphenyl)-1H-benzimidazole, **8**. Yield: 63%. Compound crystallized from EtOH to give a white solid, Mp: 175–176 °C. IR (KBr): ν_{max} 3429, 2910, 1613, 1494, 1432, 1391, 1257, 1178, 924, 835, 739 cm^{-1}. ^1H NMR (200 MHz, CD_3OD): δ 3.83 (s, 3H), 7.03 (d, J = 8,6 Hz, 2H), 7.17 (dd, J_1 = 8.6; J_2 = 1,8 Hz, 1H), 7.47 (d, J = 8.6 Hz, 1H), 7.50 (d, J = 1,8 Hz, 1H), 7.95 (d, J = 8,6 Hz, 2H). ^{13}C NMR (50 MHz, CD_3OD): δ 54.5 (O$\underline{C}H_3$), 114.0 (C-7), 114.1 (C-3′ + C-5′), 115.0 (C-4), 121.3 (C-1′), 122.6 (C-6), 127.7 (C-5), 128.0 (C-2′ + C-3′), 137.2 (C-7a), 139.6 (C-3a), 153.3 (C-2), 161.8 (C-4′). HRMS (ESI^+) calcd. for $C_{14}H_{12}ClN_2O$ $[M+H]^+$: 259.0638; found: 259.0635.

4.1.2.2.6. 5-Chloro-2-(4-chlorophenyl)-1H-benzimidazole, **9**. Yield: 80%. Compound crystallized from EtOH to give a white solid, Mp: 229–230 °C. IR (KBr): ν_{max} 3510, 2923, 1621, 1582, 1480, 1422, 1302, 1086, 925, 833, 731 cm^{-1}. ^1H NMR (200 MHz, CD_3OD): δ 7.21 (dd, J_1 = 8.6; J_2 = 2.0 Hz, 1H), 7.48 (d, J = 8.6 Hz, 1H), 7.49 (d, J = 8.6 Hz, 2H), 7.54 (d, J = 2.0 Hz, 1H), 8.00 (d, J = 8.6 Hz, 2H). ^{13}C NMR (50 MHz, CD_3OD): δ 114.4, 115.5, 123.1, 127.9 (2C), 128.2, 128.9 (2C), 136.3 (2C), 137.6, 139.8, 152.1. HRMS (ESI^+) calcd. for $C_{13}H_9Cl_2N_2$ $[M+H]^+$: 263.0143; found: 263.0143.

4.1.2.2.7. 2-(4-Methoxyphenyl)-5-nitro-1H-benzimidazole, **14**. Yield: 75%. Compound crystallized from MeOH to give a brown-red solid, Mp: 237–239 °C. IR (KBr): ν_{max} 3351, 3085, 1621, 1574, 1509, 1347, 1277, 1012, 881, 817, 737 cm^{-1}. ^1H NMR (200 MHz, C_2D_6SO): δ 3.84 (s, 3H), 7.14 (d, J = 8.8 Hz, 2H), 7.70 (d, J = 9.0 Hz, 1H), 8.08 (dd, J_1 = 9.0; J_2 = 2.4 Hz, 1H), 8.15 (d, J = 8.8 Hz, 2H), 8.40 (d, J = 2.4 Hz, 1H). ^{13}C NMR (50 MHz, C_2D_6SO): δ 55.9 (O$\underline{C}H_3$), 108.0 (C-4), 111.8 (C-7), 115.0 (C-3′ + C-5′), 118.3 (C-6), 121.8 (C-1′), 129.1 (C-2′ + C-6′), 140.3 (C-3a), 142.9 (C-5), 143.6 (C-7a), 155.8 (C-2), 161.9 (C-4′). HRMS (ESI^+) calcd. for $C_{14}H_{12}N_3O_3$ $[M+H]^+$: 270.0879, found: 270.0884.

4.1.2.2.8. 2-(4-Chlorophenyl)-5-nitro-1H-benzimidazole, **15**. Yield: 85%. Compound crystallized from MeOH to give a yellow solid, Mp: 306–307 °C. IR (KBr): ν_{max} 3441, 2921, 1601, 1498, 1333, 1289, 1060, 837, 735 cm^{-1}. ^1H NMR (200 MHz, C_2D_6SO): δ 7.67 (d, J = 8.6 Hz, 2H), 7.76 (d, J = 9.0 Hz, 1H), 8.13 (dd, J_1 = 9.0 Hz; J_2 = 2.0 Hz, 1H), 8.21 (d, J = 8.6 Hz, 2H), 8.47 (d, J = 2.0 Hz, 1H). ^{13}C NMR (50 MHz, C_2D_6SO): δ 113.1, 115.0, 118.5, 128.3, 129.0 (2C), 129.6 (2C), 136.1, 138.8, 140.2, 143.2, 155.0. HRMS (ESI^+) calcd. for $C_{13}H_9ClN_3O_2$ $[M+H]^+$: 274.0383, found: 274.0394.

4.1.2.2.9. 2-(4-Methoxyphenyl)-5,6-dimethyl-1H-benzimidazole, **23**. Yield: 60%. Compound crystallized from EtOH to give a light yellow solid, Mp: 227–229 °C. IR (KBr): ν_{max} 3435, 2921, 1612, 1500, 1440, 1384, 1253, 1151, 1031, 923, 836, 795 cm^{-1}. ^1H NMR (200 MHz, CD_3OD): δ 2.14 (s, 6H), 4.07 (s, 3H), 7.02 (d, J = 8.9 Hz, 2H), 7.33 (s, 2H), 7.92 (d, J = 8.9 Hz, 2H). ^{13}C NMR (50 MHz, CD_3OD): δ 19.5 (2 x $\underline{C}H_3$), 54.6 (O$\underline{C}H_3$), 114.0 (C-4 + C-7), 114.4 (C-3′ + C-5′), 119.7 (C-1′), 128.2 (C-2′ + C-6′), 132.8 (C-5 + C-6), 134.9 (C-3a + C-7a), 150.2 (C-2), 162.1 (C-4′). HRMS (ESI^+) calcd. for $C_{16}H_{17}N_2O$ $[M+H]^+$: 253.1341, found: 253.1352.

4.1.2.2.10. 5,6-Dichloro-2-(4-methoxyphenyl)-1H-benzimidazole, **24**. Yield: 71%. Compound crystallized from EtOH to give a beige solid, Mp: 218–220 °C. IR (KBr): ν_{max} 3321, 2939, 1610, 1573, 1492, 1383, 1261, 1192, 1090, 1028, 969, 832, 735 cm^{-1}. ^1H NMR (200 MHz, CD_3OD): δ 3.87 (s, 3H), 7.08 (d, J = 7.4 Hz, 2H), 7.69 (s, 2H), 7.99 (d, J = 7.4 Hz, 2H). ^{13}C NMR (50 MHz, CD_3OD): δ 54.6 (O$\underline{C}H_3$), 114.3 (C-3′ + C-5′), 115.4 (C-4 + C-7), 120.9 (C-1′), 125.9 (C-5 + C-6), 128.3 (C-2′ + C-6′), 138.1 (C-3a + C-7a), 154.5 (C-2), 162.2 (C-4′). HRMS (ESI^+) calcd. for $C_{14}H_{11}Cl_2N_2O$ $[M+H]^+$: 293.0248, found: 293.0238.

4.1.2.3. Method B. General procedure for the preparation of 2-phenylbenzimidazole derivatives (compounds ***3****,* ***6****,* ***7****,* ***10****,* ***11****,* ***12****,* ***16****,* ***17****,* ***20****,* ***21*** *and* ***22****).* A mixture of the corresponding 1,2-phenylenediamine (1.00 mmol), the substituted benzaldehyde (1.00 mmol) and the $Na_2S_2O_5$ (1.00 mmol) in dry DMF (4 mL) was heated to reflux for 6–12 h.

Then, the reaction was cooled to room temperature and water (20 mL) was added to provide a solid that was filtered off in Büchner. The solid was purified by column chromatography on silica gel with hexane/ethyl acetate (8:2) as elution system, and recrystallized from the adequate solvent in most cases. Reaction yields ranged within 40–73%.

4.1.2.3.1. 2-(4-Bromophenyl)-1H-benzimidazole, **3**. Yield: 40%. Compound crystallized from EtOH to give an orange solid, Mp: 295–296 °C. IR (KBr): ν_{max} 3460, 2924, 1620, 1430, 1260, 1178, 1070, 835, 802, 670 cm^{-1}. ^1H NMR (400 MHz, CD_3OD): δ 7.26 (m, 2H), 7.60 (m, 2H), 7.70 (d, J = 8.0 Hz, 2H), 7.99 (d, J = 8.0 Hz, 2H). ^{13}C NMR (100 MHz, CD_3OD): δ 124.2 (2C), 126.3, 129.5 (2C), 129.9 (2C), 130.2, 133.4 (2C), 138.9 (2C), 152.3. HRMS (ESI^+) calcd. for $C_{13}H_{10}BrN_2$ $[M+H]^+$: 273.0027, found: 273.0026.

4.1.2.3.2. 2-(2,5-Dimethylphenyl)-5-methyl-1H-benzimidazole, **6**. Yield: 42%. Compound crystallized from EtOH to give a light yellow solid, Mp: 112–113 °C. IR (KBr): ν_{max} 3430, 2920, 1629, 1447, 1276, 1000, 805 cm^{-1}. ^1H NMR (200 MHz, CD_3OD): δ 2.33 (s, 3H), 2.43 (s, 3H), 2.45 (s, 3H), 7.07 (dd, J_1 = 8.2; J_2 = 1.2 Hz, 1H), 7.18 (bs, 2H), 7.38 (m, 2H), 7.46 (d, J = 8.2 Hz, 1H). ^{13}C NMR (50 MHz, CD_3OD): δ 18.7 ($\underline{C}H_3$ at C-2′), 19.5 ($\underline{C}H_3$ at C-5′), 20.3 ($\underline{C}H_3$ at C-5), 113.8 (C-7), 114.3 (C-4), 123.8 (C-6), 129.8 (C-1′), 130.0 (C-4′), 130.2 (C-3′), 130.6 (C-6′), 132.3 (C-5), 133.8 (C-2′), 135.3 (C-5′), 136.8 (C-7a), 138.1 (C-3a), 152.4 (C-2). HRMS (ESI^+) calcd. for $C_{16}H_{17}N_2$ $[M+H]^+$: 237.1392; found: 237.1396.

4.1.2.3.3. 5-Methyl-2-(4-methoxy-3-nitrophenyl)-1H-benzimidazole, **7**. Yield: 66%. Compound crystallized from MeOH to give a yellow solid, Mp: 221–222 °C. IR (KBr): ν_{max} 3313, 2936, 1622, 1550, 1521, 1436, 1336, 1267, 1010, 815, 793 cm^{-1}. ^1H NMR (200 MHz, CD_3OD): δ 2.45 (s, 3H), 4.02 (s, 3H), 7.09 (dd, J_1 = 8.2; J_2 = 1.6 Hz, 1H), 7.35 (d, J_2 = 1.6 Hz, 1H), 7.43 (d, J = 8.6 Hz, 1H), 7.45 (d, J = 8.2 Hz, 1H), 8.25 (dd, J_1 = 8.6; J_2 = 2.4 Hz, 1H), 8.49 (d, J = 2.4 Hz, 1H). ^{13}C NMR (50 MHz, CD_3OD): δ 20.3 ($\underline{C}H_3$), 56.0 (O$\underline{C}H_3$), 112.0 (C-7), 112.2 (C-4), 114.3 (C-5′), 122.3 (C-1′), 122.9 (C-2′), 124.3 (C-6), 131.6 (C-6′), 132.4 (C-5), 136.8 (C-7a), 137.2 (C-3a), 140.0 (C-3′), 151.2 (C-2), 153.7 (C-4′). HRMS (ESI^+) calcd. for $C_{15}H_{14}N_3O_3$ $[M+H]^+$: 284.1035, found: 284.1031.

4.1.2.3.4. 5-Chloro-2-(4-nitrophenyl)-1H-benzimidazole, **10**. Yield: 55%. Compound crystallized from MeOH to give a yellow solid, Mp: 249–250 °C. IR (KBr): ν_{max} 3314, 2900, 1604, 1511, 1413, 1349, 1109, 924, 854, 809, 707 cm^{-1}. ^1H NMR (200 MHz, CD_3OD): δ 7.25 (dd, J_1 = 8.6; J_2 = 2.0 Hz, 1H), 7.56 (d, J = 8.6 Hz, 1H), 7.58 (d, J = 2.0 Hz, 1H), 8.21 (d, J = 9.0 Hz, 2H), 8.34 (d, J = 9.0 Hz, 2H). ^{13}C NMR (50 MHz, CD_3OD): δ 113.9 (C-4), 116.1 (C-7), 123.8 (C-6), 123.9 (C-3′ + C-5′), 127.3 (C-2′ + C-6′), 131.6 (C-5), 131.9 (C-7a), 135.0 (C-1′), 141.3 (C-3a), 148.7 (C-4′), 151.2 (C-2). HRMS (ESI^+) calcd. for

$C_{13}H_9ClN_3O_2$: 274.0383; found: 274.0381.

*4.1.2.3.5. 5-Chloro-2-(2,5-dimethylphenyl)-1*H*-benzimidazole,* **11**. Yield: 62%. Compound crystallized from EtOH to give a beige solid, Mp: 192–193 °C. IR (KBr): ν_{max} 3435, 2919, 1613, 1584, 1496, 1440, 1375, 1275, 1060, 926, 807 cm^{-1}. ^1H NMR (200 MHz, CD_3OD): δ 2.35 (s, 3H), 2.44 (s, 3H), 7.23 (m, 3H) 7.42 (bs, 1H), 7.57 (d, J = 8.6 Hz, 1H), 7.58 (d, J = 2.0 Hz, 1H). ^{13}C NMR (50 MHz, CD_3OD): 18.7, 19.5, 114.3, 115.4, 122.7, 127.8, 129.3, 129.9, 130.5, 130.8, 134.0, 135.5, 136.9, 139.2, 154.1. HRMS (ESI^+) calcd. for $C_{15}H_{14}ClN_2$: 257.0846; found: 257.0845.

*4.1.2.3.6. 5-Chloro-2-(4-methoxy-3-nitrophenyl)-1*H*-benzimidazole,* **12**. Yield: 70%. Compound crystallized from MeOH to give a pale yellow solid, Mp: 239–240 °C. IR (KBr): ν_{max} 3306, 2920, 1626, 1515, 1442, 1343, 1267, 1011, 923, 891, 822, 643 cm^{-1}. ^1H NMR (200 MHz, C_2D_6SO): δ 4.00 (s, 3H), 7.21 (dd, J_1 = 8.6; J_2 = 2.4 Hz, 1H), 7.56 (d, J = 9.0 Hz, 1H), 7.60 (d, J = 8.6 Hz, 1H), 7.63 (d, J = 2.4 Hz, 1H), 8.42 (d, J_1 = 9.0; J_2 = 2.2 Hz, 1H), 8.64 (d, J = 2.2 Hz, 1H). ^{13}C NMR (50 MHz, C_2D_6SO): δ 57.5, 115.2, 115.6, 116.4, 122.6, 123.0, 123.6, 127.0, 132.9, 138.4, 139.6, 140.9, 151.1, 153.8. HRMS (ESI^+) calcd. for $C_{14}H_{11}ClN_3O_3$: 304.0489; found: 304.0478.

*4.1.2.3.7. 2-(2,5-Dimethylphenyl)-5-nitro-1*H*-benzimidazole,* **16**. Yield: 58%. Compound crystallized from MeOH to give a white solid, Mp: 257–258 °C. IR (KBr): ν_{max} 3420, 2923, 1626, 1510, 1469, 1334, 1287, 1065, 921, 884, 737 cm^{-1}. ^1H NMR (200 MHz, CD_3OD): δ 2.33 (s, 3H), 2.45 (s, 3H), 7.19 (d, J = 8.6 Hz, 1H), 7.21 (d, J = 8.6, 1H), 7.42 (s, 1H), 7.62 (d, J = 8.6 Hz, 1H), 8.09 (dd, J_1 = 8.6; J_2 = 2.0 Hz, 1H), 8.41 (d, J = 2.0 Hz, 1H). ^{13}C NMR (50 MHz, CD_3OD): δ 18.9, 19.5, 112.1, 114.0, 117.9, 128.6, 129.9, 131.0 (2C), 134.2, 135.6, 140.1, 141.9, 143.4, 157.2. HRMS (ESI^+) calcd. for $C_{15}H_{14}N_3O_2$ $[M+H]^+$: 268.1086; found: 268.1080.

*4.1.2.3.8. 2-(4-Methoxy-3-nitrophenyl)-5-nitro-1*H*-benzimidazole,* **17**. Yield: 43%. Compound crystallized from MeOH to give a dark yellow solid, Mp: 290–292 °C. IR (KBr): ν_{max} 3433, 3351, 2923, 1621, 1508, 1444, 1347, 1277, 1066, 1012, 881, 817, 736 cm^{-1}. ^1H NMR (200 MHz, C_2D_6SO): δ 4.02 (s, 3H), 7.61 (d, J = 9.0 Hz, 1H), 7.76 (d, J = 9.0 Hz, 1H), 8.12 (dd, J_1 = 9.0; J_2 = 2.4 Hz, 1H), 8.44 (d, J = 2.4 Hz, 1H), 8.46 (dd, J_1 = 9.0; J_2 = 2.4 Hz, 1H), 8.70 (d, J = 2.4 Hz, 1H). ^{13}C NMR (50 MHz, C_2D_6SO): δ 57.2, 113.0113.7, 115.3, 118.2, 121.4, 123.7, 132.9, 137.9, 139.1, 142.8, 145.3, 153.9, 154.0. HRMS (ESI^+) calcd. for $C_{14}H_{11}N_4O_5$ $[M+H]^+$: 315.0729; found: 315.0718.

*4.1.2.3.9. 5-Methoxy-2-(4-methoxyphenyl)-1*H*-benzimidazole,* **20**. Yield: 46%. Compound crystallized from EtOH to give a yellow solid, Mp: 150–152 °C. IR (KBr): ν_{max} 3350, 2920, 1623, 1512, 1430, 1335, 1330, 1285, 1220, 1060, 920, 818, 795 cm^{-1}. ^1H NMR (400 MHz, CD_3OD): δ 3.87 (s, 3H), 3.89 (s, 3H), 7.00 (dd, J_1 = 9.2; J_2 = 2.0 Hz, 1H), 7.12 (d, J = 2.0 Hz, 1H), 7.13 (d, J = 8.4 Hz, 2H), 7.52 (d, J = 9.2 Hz, 1H), 7.99 (d, J = 8.4 Hz, 2H). ^{13}C NMR (100 MHz, CD_3OD): δ 54.7 ($O\underline{C}H_3$), 54.9 ($O\underline{C}H_3$), 96.2 (C-4), 113.5 (C-6), 114.2 (C-7), 114.6 (C-3′ + C-5′), 118.9 (C-1′), 128.3 (C-2′ + C-6′) 130.4 (C-7a), 136.2 (C-3a), 150.5 (C-2), 157.7 (C-5), 162.5 (C-4′). HRMS (ESI^+) calcd. for $C_{15}H_{15}N_2O_2$ $[M+H]^+$: 255.1134, found: 255.1122.

*4.1.2.3.10. 2-(4-Chlorophenyl)-5-methoxy-1*H*-benzimidazole,* **21**. Yield: 65%. Compound crystallized from EtOH to give a yellow solid, Mp: 227–228 °C. IR (KBr): ν_{max} 3350, 2910, 1635, 1595, 1424, 1330, 1271, 1158, 1032, 966, 825, 724 cm^{-1}. ^1H NMR (200 MHz, CD_3OD): δ 3.84 (s, 3H), 6.90 (dd, J_1 = 8.6; J_2 = 2.2Hz, 1H), 7.07 (d, J = 2.2 Hz, 1H), 7.47 (d, J = 8.6 Hz, 1H), 7.51 (d, J = 8.6 Hz, 2H), 7.99 (d, J = 8.6 Hz, 2H). ^{13}C NMR (50 MHz, CD_3OD): δ 56.1, 97.8, 113.9, 117.0, 128.9 (2C), 129.9, 130.2 (2C), 136.9, 139.0, 142.2, 151.6, 158.4. HRMS (ESI^+) calcd. for $C_{14}H_{12}ClN_2O$ $[M+H]^+$: 259.0638, found: 259.0636.

*4.1.2.3.11. 2-(4-Bromophenyl)-5-methoxy-1*H*-benzimidazole,* **22**. Yield: 73%. IR (KBr): ν_{max} 3300, 2910, 1635, 1595, 1424, 1330, 1271, 1158, 1023, 966, 825, 724 cm^{-1}. ^1H NMR (400 MHz, CD_3OD): δ 3.85 (s, 3H), 6.90 (dd, J_1 = 8.8; J_2 = 1.6 Hz, 1H), 7.08 (d, J = 1.6 Hz, 1H), 7.49 (d, J = 8.8 Hz, 1H), 7.69 (d, J = 7.6 Hz, 2H), 7.95 (d, J = 7.6 Hz, 2H). ^{13}C NMR (100 MHz, CD_3OD): δ 54.7, 96.4, 112.6, 115.6, 123.7, 127.7 (2C), 128.8, 131.8 (2C), 136.0, 138.8, 150.3, 157.1. HRMS (ESI^+) calcd. for $C_{14}H_{12}BrN_2O$ $[M+H]^+$: 303.0133, found: 303.0128.

4.1.2.4. Procedure for the reduction of nitrobenzimidazoles (compounds ***13*** *and* ***18****).* A solution with 0.32 mmol of the nitrobenzimidazole in MeOH (3 mL) in a two-necked round bottom flask was prepared, then Pd–C catalyst (3 mg) was added. The air was removed, and a balloon with H_2 was attached to one of the necks. The mixture was kept at room temperature and under magnetic stirring for 2 h. Then, the Pd–C was removed by filtration through Celite, and the residue was washed with MeOH. The solvent was removed *in vacuo* to provide a dark yellow solid.

*4.1.2.4.1. 5-Chloro-2-(3-amino-4-methoxyphenyl)-1*H*-benzimidazole,* **13**. Yield: 91%. Compound crystallized from MeOH to give a light yellow solid, Mp: 185–186 °C. IR (KBr): ν_{max} 3306, 3210, 2918, 1618, 1501, 1453, 1340, 1243, 1026, 927, 802 cm^{-1}. ^1H NMR (200 MHz, CD_3OD): δ 3.91 (s, 3H), 6.96 (d, J = 8.2 Hz, 1H), 7.20 (dd, J_1 = 8.6; J_2 = 1.6 Hz, 1H), 7.38 (dd, J_1 = 8.2; J_2 = 2.0 Hz, 1H), 7.42 (d, J = 2.0 Hz, 1H), 7.49 (d, J = 8.6 Hz, 1H), 7.52 (d, J = 1.6 Hz, 1H). ^{13}C NMR (50 MHz, CD_3OD): δ 54.7, 110.0, 112.7, 113.9, 114.9, 117.0, 121.6, 122.4, 127.6, 137.3, 139.8, 140.0, 149.7, 154.0. HRMS (ESI^+) calcd. for $C_{14}H_{13}ClN_3O$: 274,0747, found: 304.0735.

*4.1.2.4.2. 5-Amino-2-(4-methoxyphenyl)-1*H*-benzimidazole,* **18**. Yield: 65%. Compound crystallized from MeOH to give a brown-red solid, Mp: 195–197 °C. IR (KBr): ν_{max} 3300, 2910, 1626, 1573, 1355, 1330, 1267, 1011, 923, 820, 795 cm^{-1}. ^1H NMR (200 MHz, CD_3OD): δ 3.84 (s, 3H), 6.73 (dd, J_1 = 8.6; J_2 = 1.8 Hz, 1H), 6.92 (d, J = 1.8 Hz, 1H), 7.03 (d, J = 9.0 Hz, 2H), 7.35 (d, J = 8.6 Hz, 1H), 7.94 (d, J = 9.0 Hz, 2H). ^{13}C NMR (50 MHz, CD_3OD): δ 54.4 ($O\underline{C}H_3$), 99.0 (C-4), 112.9 (C-6), 113.9 (C-3′ + C-5′), 115.4 (C-7), 122.3 (C-1′), 127.4 (C-2′ + C-6′), 133.9 (C-7a), 138.5 (C-3a), 143.1 (C-5), 150.9 (C-2), 161.0 (C-4′). HRMS (ESI^+) calcd. for $C_{14}H_{14}N_3O$ $[M+H]^+$: 240.1137, found: 240.1131.

4.1.2.5. Coupling of BZ **18** *with picolinic acid,* **19**. 79 mg (0.49 mmol) of 1,1-carbonildiimidazole (CDI) was added to a solution of 50 mg (0.41 mmol) of picolinic acid in dry DMF (2 mL), and the mixture was maintained at room temperature for 1 h. Then, 88 mg (0.37 mmol) of compound BZ **18** was added, and the mixture was kept at room temperature with magnetic stirring for 16 h. The progress of the reaction was monitored by TLC, and a mixture of *n*-hexane/ethyl acetate (1:9) was used as eluent. After completion of the reaction, the solvent was removed under *vacuum* on a rotary evaporator, and the solid purified by column chromatography with *n*-hexane/ethyl acetate (2:8) as eluent gave 40 mg (67% yield) of an orange solid.

*4.1.2.4.3. 2-(4-Methoxyphenyl)-5-picolinamidil-1*H*-benzimidazole,* **19**. Yield: 70%. IR (KBr): ν_{max} 3300, 2910, 1626, 1573, 1355, 1330, 1267, 1011, 923, 820, 795 cm^{-1}. ^1H NMR (400 MHz, CD_3OD): δ 3.88 (s, 3H), 7.09 (d, J = 8.0 Hz, 2H), 7.50 (dd, J_1 = 8.6; J_2 = 1.8 Hz, 1H), 7.58 (d, J = 8.6 Hz, 1H), 7.62 (m, 1H), 8.03 (d, J = 8.0 Hz, 2H), 8.04 (d, J = 1.8 Hz, 1H), 8.23 (m, 1H), 8.29 (m, 1H), 8.73 (m, 1H)· ^{13}C NMR (100 MHz, CD_3OD): δ 55.9 ($O\underline{C}H_3$), 107.1 (C-4), 115.6 (C-3′ + C-5′), 116.2 (C-7), 117.7 (C-6), 123.1 (C-1′), 123.3 (C-3″), 127.9 (C-5″), 129.4 (C-2′ + C-6′), 134.6 (C-5), 139.1 (C-4″), 139.2 (C-3a), 140.1 (C-7a), 149.7 (C-6″), 151.2 (C-2″), 154.2 (C-2), 163.1 (C-4′), 164.4 ($\underline{C}$ONH). HRMS (ESI^+) calcd. for $C_{20}H_{17}N_4O_2$ $[M+H]^+$: 345,1352, found: 345.1340.

4.2. Biological evaluation

4.2.1. Chemicals and drugs

Stock solutions of all the compounds and positive controls were prepared in DMSO (Sigma 276855), while the final dilutions were made with distilled water in order to maintain a maximum

concentration of 0.5% DMSO per well. To perform the different *in vitro* tests, thiabendazole (TBZ, Sigma T8904) or ivermectin (IVM, Sigma I8898) were used as positive controls, while 0.5% DMSO was used as negative control in all tests. Levamisole (LEV, Sigma 31742) was also used as positive control but in this case, the stock solution was prepared in distilled water.

4.2.2. Teladorsagia circumcincta

Different *in vitro* tests were carried out to test the anthelmintic activity of the new compounds in three stages of the parasite: eggs, first stage larvae (L1) and third stage larvae (L3). All of these tests were performed using two different strains, one susceptible and one resistant to BZs, LEV and IVM (the latter kindly provided by Dr. Dave Bartle, Moredun Research Institute, Edinburgh, UK).

4.2.3. Animals

To obtain biological material for further experiments, six 3 months-old Merino lambs were infected with 25,000 L3 of *T. circumcincta* at the facilities of the "Instituto de Ganadería de Montaña" (León, Spain). As indicated above, four of them were infected with a susceptible strain and the other two with the resistant one. All study protocols were revised and approved by the University of León Animal Care Committee (León, Spain) to AGL2016-79813-C2-1R/2R, according to current national and European regulations of animal wellbeing (R.D 53/2013 and EU Directive 2010/63/EU).

4.2.4. In vitro tests

A total of three *in vitro* experiments were undertaken to determine the activity of the 24 BZ derivatives against different stages of *T. circumcincta* using a susceptible strain of the parasite. An initial screening of the compounds was performed using a first discriminant concentration of 50 μM by the Egg Hatch Test (EHT), and the Larval Migration Inhibition Test (LMIT). The next step was to calculate the half maximal effective concentration (EC_{50}) in those compounds with activities higher than 90% at this initial screening. Then, with those compounds, the same initial screening at a discriminant dose of 50 μM within a resistant strain of the parasite was performed, and as in the previous case, EC_{50} was later calculated in those compounds with efficacies higher than 80%. When the EHT was carried out, some compounds showed larvicidal activity, so a Larval Mortality Test (LMT) was also performed in parallel. The procedure in this case was the same as in the EHT: an initial screening at a discriminant dose of 50 μM and the estimation of their EC_{50}.

All compounds were tested at least in duplicate at 3 different days to accurate the results.

Cytotoxicity assays were conducted on human Caco-2 and HepG2 cell lines with the aim to define the Selectivity Indexes (SI) for those compounds in which the EC_{50} was determined, and to compare the SI with those of the reference drug thiabendazole (TBZ).

4.2.4.1. Egg hatching test (EHT). EHT is based on a modification of a protocol previously described by Ref. [31]. Briefly, parasite eggs were freshly obtained from lamb faeces experimentally infected with *T. circumcincta* and distributed in 24-well cell culture plates (Costar®, CLS3738) at a density of 100–150 eggs per well in a volume of 1 mL. To carry out the initial testing, a 10 mM stock solution was prepared by dissolving each compound in DMSO, from which working solutions were prepared by further dilutions with distilled water. Each well included 1 mL of the egg suspension, 10 μL of a stock solution with each compound and distilled water up to 2 mL to achieve a final concentration in well of 50 μM. Additionally, in each plate TBZ was included at concentration of 0.1 μg/mL (0.5 μM) as positive control. After 48 h incubation at 23 °C, the number of L1 and eggs present per well were counted using an inverted microscope to determine the percentage of hatched eggs (number of L1/number of L1 larvae and eggs X 100). The ovicidal activity was expressed by the percentage of egg hatching inhibition using the following formula:

% Egg hatching inhibition = [100 − (% egg hatching per well/% egg hatching in control well)] x 100.

The EC_{50} of the compounds was calculated using 6 concentrations ranging from 50 μM to 1.56 μM.

4.2.4.2. Larval mortality test (LMT). This test was carried out only on those compounds in which dead larvae appeared during the EHT reading (BZs **4**, **9** and **22**), in order to discard a possible activity against this parasite stage.

With the aim to obtain L1, fresh eggs (previously extracted from the faeces) were incubated during 24 h at 23 °C. Then, larvae were collected in a known volume of water to obtain a density of 100–150 larvae per mL. The LMT was performed in the same way as the EHT but using the L1 instead. In this case a stock solution of LEV at 10 mg/mL was added as positive control on every plate to reach a final concentration of 1 mg/mL (4.15 mM) per well. The number of dead and alive L1 present per well was counted using an inverted microscope to determine the larvicidal activity of the compound ([number of dead L1/number of dead and alive L1] X 100). Apparently motionless and rod-shaped larvae were considered dead, while those that presented some kind of movement or curvature in their body were considered alive. The efficacy of the compound was expressed by the percentage of viability inhibition using the following formula:

% Viability inhibition = (% larvicidal activity per well/% larvicidal activity in control well) x 100.

The EC_{50} of each compound was calculated using 6 concentrations ranging from 50 μM to 1.56 μM.

4.2.4.3. Larval migration inhibition test (LMIT). LMIT was conducted in following the method described previously by Ref. [32]. To obtain L3, faeces from infected lambs were cultured in aerated and humidified closed boxes twice a week and placed in a climatic chamber at 25 °C for 13 days. Briefly, L3 were exsheathed by incubation in 0.5% (v/v) sodium hypochlorite solution for 10 min at room temperature. After incubation, the larvae suspension was washed 3 times by adding distilled water and centrifugation for 15 min at 300 g. Then, the number of larvae was adjusted to a density of 1000 L3 per mL and aliquots of 100 μL were added to each well in a 96-well culture plate (VWR, 734–2327) containing 100 μL of a suspension of distilled water with the compounds. As in the other test, all compounds were tested at a single dose of 50 μM; and 100 μM final concentration IVM was used as positive control. Each compound was tested in triplicate on the same plate and at least two technical replicas were performed. After 24 h of incubation in the dark at 28 °C, the whole content of each well was transferred to a 96-wells MultiScreen-Mesh Filter Plate (Sigma-Aldrich, MANMN2010) and left for a further 24 h to allow the motile L3 to pass through the sieves (20 μm mesh size) for counting. The size of the mesh was 20 μm to prevent the "fall" of the larvae since the cross-diameter of these is slightly larger [33].

The efficacy was expressed by the percentage of larval migration inhibition using the following formula:

% Larval migration inhibition = [(number of larvae migrating through sieves in negative controls wells − number of larvae

migrating through sieves in treatment wells) / number of larvae migrating through sieves in negative controls wells.] x 100

The EC_{50} of each compound was calculated using 6 concentrations ranging from 50 μM to 1.56 μM.

4.2.5. Cytotoxicity assay and selectivity indexes

The cytotoxicity evaluation of 2-phenylbenzimidazoles was carried out on two human cell lines: the colorectal adenocarcinoma Caco-2 (ATCC® HTB-37™) and the hepatocarcinoma HepG2 (ATCC® HB-8065™). Briefly, 10,000 cells were seeded on 96 well-plates in RPMI 1640 Medium supplemented with 2.0 g/L sodium bicarbonate (Fisher Scientific®), 1% (w/v) L-glutamine (Sigma-Aldrich®), and 25 mM HEPES buffer, 10% (v/v) inactivated foetal bovine serum (FBS), and antibiotic mixture containing 10,000 U/mL penicillin and 10,000 μg/mL streptomycin. Cultures were incubated at 37 °C in a humidified atmosphere containing 5% CO_2. After 24 h, different concentrations of testing compounds (ranging from 1 to 100 μM) were added for 72 h. After this time, the viability of the cells was assessed using the Alamar Blue (BioRad) staining method according to manufacturer's recommendations (Invitrogen).

Cytotoxic concentration 50 (CC_{50}) values were determined by plotting the concentration of each compound *vs*. cell viability expressed as the fluorescence emitted by resorufin at 590 nm. Dose-response curves were fitted using non-linear regression plots, using Sigma Plot programme (10.0 Software, Inc., San José, California; USA).

As a safety parameter of each compound, selectivity index (SI) was calculated as the CC_{50}/EC_{50} ratio of those compounds with a measurable effect on eggs or larvae. Despite the fact that the SI was calculated using non-congruent magnitudes (cells *vs* organisms), we considered that it was useful to compare the relative toxicity of the compounds.

4.2.6. Predictive drug-likeness and ADME-Toxicity parameters for BZs

Compounds with the best nematocidal activity and weak cytotoxicity were submitted to *in silico* pharmacokinetic properties and adverse effects prediction. To predict the druggability of these compounds, we got the parameters (see supplementary data) related to Lipinski's rule of five, absorption rate, drug-likeness and potential toxicity risks provided online by the freely accessible web-based applications Osiris Data Warrior (http://www.openmolecules.org/datawarrior and https://www.organic-chemistry.org/prog/peo); and preADMET (https://preadmet.bmdrc.kr/adme/and https://preadmet.bmdrc.kr/druglikeness/).

4.2.7. Tubulin homology modelling

Homology modelling of *T. circumcincta* β-tubulin was performed with SWISS-MODEL Workspace [34]. The sequence of this protein was taken from the one published in the literature [35]. This protein has a highly conserved region, which includes the most representative amino acids of the active site. This conserved region was identified after comparison with other β-tubulin sequence species using GCG software. Residues 1–419 of chain B of the crystallographic structure of *Ovis aries* tubulin (PDB ID: 3N2G) were used as a template [36].

The protein structure was validated by the use of Rampage server (http://mordred.bioc.cam.ac.uk/~rapper/rampage.php) which predict the stereochemical quality and accuracy of the generated model. Ramachandran plot analysis revealed 92.7% residues of modelled structure in the favoured region, 6.0% residues in the allowed region, and 1.3% residues in the disallowed region.

4.2.8. Molecular docking

Docking calculations were performed using Glide integrated into the Schrödinger Molecular Modelling Suite (Schrödinger, Inc., USA, 2016–4). *T. circumcinta* β-tubulin previously obtained by homology modelling was used as a target to further understand the molecular bases of the inhibitory properties of these compounds. This target was processed with the Protein Preparation Wizard available in the modelling package. The process preparation of the protein included assignation of bond orders, addition and optimization of hydrogens, filling in missing side chains, cap termini addition, optimization of protonation states of some residues, H-bond network optimization, etc. The model was refined using OPLS-2005 Force Field. The ligands which appear in Table 1 were processed with the LigPrep module implemented in the same package previous to optimizing the structure of each ligand; afterwards different tautomers were generated considering the different protonation states (pH 7.0 ± 2.0) and partial charges using the OPLS-2005 force-field were assigned.

A receptor grid was generated and centred in the colchicine binding site of the β-tubulin. The size of the box was 25x25x25 Å, with a van der Waals scaling factor of 1.0 and a partial charge cut-off of 0.25. Docking was carried out using the Extra Precision (XP) mode of Glide. The final pose was selected using the energetic parameter GlideScore function. The docking poses of some significant ligands can be visualized and analysed for the key elements of interaction with the target enzyme using the Maestro's Pose Viewer utility in Figs. 1–4 and supplementary material (section 4).

Author contributions

All authors participate in their respective areas of research and collaborate to the writing of the manuscript.

Declaration of competing interest

The authors declare that they have no known competing financial interests or personal relationships that could have appeared to influence the work reported in this paper.

Acknowledgements

We would like to express our gratitude to Dr. Dave Bartley at Moredun Research Institute for providing the triple-resistant strain of *T. circumcincta*. Authors thank Bioinformatic & Molecular Design Research Centre (BMDRC, Yonsey University, Seoul, Korea) and Idorsia Pharmaceuticals Ltd. (Allschwil, Switzerland) for complimentary access to preADMET and Osiris Data Warrior databases, respectively. RE thanks financiation from RICET-USAL Program RD16/0027/0018. Financial support came from MINECO: RETOS (AGL2016-79813-C2-1R/2R) and Junta de Castilla y León co-financed by FEDER, UE (LE020P17). EVG was funded by FPU16/03536, VCGA by Junta de Castilla y León and FSE (LE082-18), MAV by Junta de Castilla y León (LE051-18) and MMV by the Spanish "Ramon y Cajal" Programme (Ministerio de Economía y Competitividad; MMV, RYC-2015-18368), respectively.

Appendix A. Supplementary data

Supplementary data to this article can be found online at https://doi.org/10.1016/j.ejmech.2020.112554.

References

[1] World Health Organization, Schistosomiasis and Soiltransmitted Helminthiases: Numbers of People Treated in 2017 [WWW Document], vol. 93, 2018.

WHO. URL, http://www.who.int/wer2018. accessed 7.18.2019.
[2] P.J. Hotez, Aboriginal populations and their neglected tropical diseases, PLoS Neglected Trop. Dis. 8 (2014), e2286, https://doi.org/10.1371/journal.pntd.0002286.
[3] S.P. Montgomery, M.C. Starr, Soil-transmitted helminthiasis in the United States: a systematic review—1940–2010, Am. J. Trop. Med. Hyg. 85 (2011) 680–684, https://doi.org/10.4269/ajtmh.2011.11-0214.
[4] F. Schär, U. Trostdorf, F. Giardina, V. Khieu, S. Muth, H. Marti, P. Vounatsou, P. Odermatt, *Strongyloides stercoralis*: global distribution and risk factors, PLoS Neglected Trop. Dis. 7 (2013) e2288, https://doi.org/10.1371/journal.pntd.0002288.
[5] M.A. Cruz-Rojo, M. Martínez-Valladares, M.A. Álvarez-Sánchez, F.A. Rojo-Vázquez, Effect of infection with *Teladorsagia circumcincta* on milk production and composition in Assaf dairy sheep, Vet. Parasitol. 185 (2012) 194–200, https://doi.org/10.1016/j.vetpar.2011.10.023.
[6] A. Kloosterman, H.K. Parmentier, H.W. Ploeger, Breeding cattle and sheep for resistance to gastrointestinal nematodes, Parasitol. Today 8 (1992) 330–335, https://doi.org/10.1016/0169-4758(92)90066-B.
[7] A.R. Sykes, Parasitism and production in farm animals, Anim. Sci. 59 (1994) 155–172, https://doi.org/10.1017/S0003356100007649.
[8] F. Jackson, R.L. Coop, The development of anthelmintic resistance in sheep nematodes, Parasitology 120 (2000) 95–107, https://doi.org/10.1017/S0031182099005740.
[9] R.M. Kaplan, Drug resistance in nematodes of veterinary importance: a status report, Trends Parasitol. 20 (2004) 477–481, https://doi.org/10.1016/J.PT.2004.08.001.
[10] E. Papadopoulos, E. Gallidis, S. Ptochos, Anthelmintic resistance in sheep in Europe: a selected review, Vet. Parasitol. 189 (2012) 85–88, https://doi.org/10.1016/j.vetpar.2012.03.036.
[11] M. Abongwa, R.J. Martin, A.P. Robertson, A brief review on the mode of action of antinematodal drugs, Acta Vet. 67 (2017) 137–152, https://doi.org/10.1515/acve-2017-0013.
[12] D.B. Bhinsara, M. Sankar, D.N. Desai, J.J. Hasnani, P.V. Patel, N.D. Hirani, V.D. Chauhan, Benzimidazole resistance: an overview, Int. J. Curr. Microbiol. App. Sci 7 (2018) 3091–3104, https://doi.org/10.20546/ijcmas.2018.702.372.
[13] L.F.V. Furtado, A.C.P. de Paiva Bello, E.M.L. Rabelo, Benzimidazole resistance in helminths: from problem to diagnosis, Acta Trop. 162 (2016) 95–102, https://doi.org/10.1016/j.actatropica.2016.06.021.
[14] M. Martínez-Valladares, T. Geurden, D.J. Bartram, J.M. Martínez-Pérez, D. Robles-Pérez, A. Bohórquez, E. Florez, A. Meana, F.A. Rojo-Vázquez, Resistance of gastrointestinal nematodes to the most commonly used anthelmintics in sheep, cattle and horses in Spain, Vet. Parasitol. 211 (2015) 228–233, https://doi.org/10.1016/j.vetpar.2015.05.024.
[15] J. Vercruysse, M. Albonico, J.M. Behnke, A.C. Kotze, R.K. Prichard, J.S. McCarthy, A. Montresor, B. Levecke, Is anthelmintic resistance a concern for the control of human soil-transmitted helminths? Int. J. Parasitol. Drugs Drug Resist. 1 (2011) 14–27, https://doi.org/10.1016/j.ijpddr.2011.09.002.
[16] S.K. Tahir, P. Kovar, S.H. Rosenberg, S.C. Ng, Rapid colchicine competition binding scintillation proximity assay using biotin-labelled tubulin, Biotechniques 29 (2000) 156–160, https://doi.org/10.2144/00291rr02.
[17] R. Aguayo-Ortiz, O. Méndez-Lucio, J.L. Medina-Franco, R. Castillo, L. Yépez-Mulia, F. Hernández-Luis, A. Hernández-Campos, Towards the identification of the binding site of benzimidazoles to β-tubulin of *Trichinella spiralis*: insights from computational and experimental data, J. Mol. Graph. Model. 41 (2013) 12–19, https://doi.org/10.1016/j.jmgm.2013.01.007.
[18] R.N. Beech, P. Skuce, D.J. Bartley, R.J. Martin, R.K. Prichard, S. Gilleard, Anthelmintic resistance: markers for resistance or susceptibility? Parasitology 138 (2010) 160–174, https://doi.org/10.1017/S0031182010001198.
[19] W. Wang, D. Kong, H. Cheng, L. Tan, Z. Zhang, X. Zhuang, H. Long, Y. Zhou, Y. Xu, X. Yang, K. Ding, New benzimidazole-2-urea derivatives as tubulin inhibitors have been reported, Bioorg. Med. Chem. Lett 24 (2014) 4250–4253, https://doi.org/10.1016/j.bmcl.2014.07.035.
[20] G.A. Patani, E.J. LaVoie Bioisosterism, A Rational approach in drug design, Chem. Rev. 96 (1996) 3147–3176, https://doi.org/10.1021/cr950066q.
[21] M. Zajíčková, L.T. Nguyen, L. Skálová, L. Raisová Stuchlíková, P. Matoušková, Anthelmintics in the future: current trends in the discovery and development of new drugs against gastrointestinal nematodes, Drug Discov. Today 25 (2020) 430–437, https://doi.org/10.1016/j.drudis.2019.12.007.
[22] M. Tonelli, M. Simone, B. Tasso, F. Novelli, V. Boido, F. Sparatore, G. Paglietti, S. Prici, G. Giliberti, S. Blois, C. Ibba, G. Sanna, R. Laddo, P.L. Colla, Antiviral activity of benzimidazole derivatives II antiviral activity of 2-phenylbenzimidazole derivatives, Bioorg. Med. Chem. 18 (2010) 2937–2953, https://doi.org/10.1016/j.bmc.2010.02.037.
[23] M. Tonelli, F. Novelli, B. Tasso, I. Vazzana, A. Sparatore, V. Boido, F. Sparatore, P.L. Colla, G. Sanna, G. Giliberti, B. Busonera, P. Farci, C. Ibba, R. Loddo, Antiviral activity of benzimidazole derivatives. III. Novel anti-CVB-5, anti-RSV and anti-Sb-1 agents, Bioorg. Med. Chem. 22 (2014) 4893–4909, https://doi.org/10.1016/j.bmc.2014.06.043.
[24] S. Utku, M. Topal, A. Dögen, M.S. Serin, Synthesis, characterization, antibacterial and antifungal evaluation of some new platinum(II) complexes of 2-phenylbenzimidazole ligands, Turk. J. Chem. 34 (2010) 427–436, https://doi.org/10.3906/kim-1002-5.
[25] R. Sawant, D. Kawade, Synthesis and biological evaluation of some novel 2-phenyl benzimidazole-1-acetamide derivatives as potential anthelmintic agents, Acta Pharm. 61 (2011) 353–361, https://doi.org/10.2478/v10007-011-0029-z.
[26] E.R. Morgan, J. van Dijk, Climate and the epidemiology of gastrointestinal nematode infections of sheep in Europe, Vet. Parasitol. 189 (2012) 8–14, https://doi.org/10.1016/j.vetpar.2012.03.028.
[27] A. Shaukat, H.M. Mirza, A.H. Ansari, M. Yasinzai, S.Z. Zaidi, S. Dilshad, F.L. Ansari, Benzimidazole derivatives: synthesis, leishmanicidal effectiveness and molecular docking studies, Med. Chem. Res. 22 (2012) 3606–3620, https://doi.org/10.1007/S00044-012-0375-5.
[28] R. Sawant, D. Kawade, Synthesis and biological evaluation of some novel 2-phenyl benzimidazole-1-acetamide derivatives as potential anthelmintic agents, Acta Pharm. 61 (2011) 353–361, https://doi.org/10.2478/v10007-011-0029-z.
[29] J.G. Penieres-Carrillo, H. Ríos-Guerra, J. Pérez-Flores, B. Rodríguez-Molina, A. Torres-Reyes, F. Barrera-Téllez, J. González-Carrillo, L. Moreno-González, A. Martínez-Zaldívar, J.J. Nolasco-Fidencio, A.S. Matus-Meza, R.A. Luna-Mora, Reevaluating the synthesis of 2,5-disubstituted-1*H*-benzimidazole derivatives by different green activation techniques and their biological activity as antifungal and antimicrobial inhibitor, J. Heterocycl. Chem. 57 (2020) 436–455, https://doi.org/10.1002/jhet.3801.
[30] W.L.F. Armarego, D.D. Perrin, Purification of Laboratory Chemicals, fourth ed., Butterworth-Heinemann, Oxford. MA, 1997.
[31] G.C. Coles, C. Bauer, F.H.M. Borgsteede, S. Geerts, T.R. Klei, M.A. Taylor, P.J. Waller, World Association for the Advancement of Veterinary Parasitology (W.A.A.V.P.) methods for the detection of anthelmintic resistance in nematodes of veterinary importance, Vet. Parasitol. 44 (1992) 35–44, https://doi.org/10.1016/0304-4017(92)90141-U.
[32] J. Demeler, U. Küttler, G. von Samson-Himmelstjerna, Adaptation and evaluation of three different in vitro tests for the detection of resistance to anthelmintics in gastro intestinal nematodes of cattle, Vet. Parasitol. 170 (2010) 61–70, https://doi.org/10.1016/j.vetpar.2010.01.032.
[33] B. Rabel, R. Mcgregor, P.G.C. Douch, Improved bioassay for estimation of inhibitory effects of ovine gastrointestinal mucus and anthelmintics on nematode larval migration, Int. J. Parasitol. 24 (1994) 671–676, https://doi.org/10.1016/0020-7519(94)90119-8.
[34] A. Waterhouse, M. Bertoni, S. Bienert, G. Studer, G. Tauriello, R. Gumienny, F.T. Heer, T.A.P. de Beer, C. Rempfer, L. Bordoli, R. Lepore, T. Schwede, Swiss-Model, Homology modelling of protein structures and complexes, Nucleic Acids Res. 46 (2018) W296–W303, https://doi.org/10.1093/nar/gky427.
[35] L. Elard, A.M. Comes, J.F. Humbert, Sequences of beta-tubulin cDNA from benzimidazole-susceptible and -resistant strains of *Teladorsagia circumcincta*, a nematode parasite of small ruminants, Mol. Biochem. Parasitol. 79 (1996) 249–253, https://doi.org/10.1016/0166-6851(96)02664-3.
[36] P. Barbier, A. Dorleans, F. Devred, L. Sanz, D. Allegro, C. Alfonso, M. Knossow, V. Peyrot, J.M. Andreu, Stathmin and interfacial microtubule inhibitors recognize a naturally curved conformation of tubulin dimers, J. Biol. Chem. 285 (2010) 31672–31681, https://doi.org/10.1074/jbc.M110.141929.